

Third harmonic generation at 223 nm in the metallic regime of GaP

V. Roppo,^{1,2,a)} J. V. Foreman,² N. Akozbek,² M. A. Vincenti,³ and M. Scalora²

¹DFEN, Universitat Politècnica de Catalunya, Rambla Sant Nebridi, 08222 Terrassa, Spain

²Charles M. Bowden Research Center, RDECOM, Redstone Arsenal, Alabama 35898-5000, USA

³AEGIS Technologies Group, 410 Jan Davis Drive, Huntsville, Alabama 35806, USA

(Received 5 January 2011; accepted 20 February 2011; published online 14 March 2011)

We demonstrate second and third harmonic generation from a GaP substrate 500 μm thick. The second harmonic field is tuned at the absorption resonance at 335 nm, and the third harmonic signal is tuned at 223 nm, in a range where the dielectric function is negative. These results show that a phase locking mechanism that triggers transparency at the harmonic wavelengths persists regardless of the dispersive properties of the medium, and that the fields propagate hundreds of microns without being absorbed even when the harmonics are tuned to portions of the spectrum that display metallic behavior. © 2011 American Institute of Physics. [doi:10.1063/1.3565240]

The solutions of Maxwell's equations in nonlinear dielectrics that display second harmonic generation (SHG) have been thoroughly studied since the early 1960s.¹ In the undepleted pump regime the solution is composed of two parts: one solves the homogeneous equation; the other is a particular solution of the inhomogeneous equation driven by the nonlinear polarization term. Observations of a double-peaked SH signal in the strong phase mismatched regime have been reported.^{2,3} In Ref. 4 the predictions made in Ref. 1 were verified, i.e., that the inhomogeneous component of the second harmonic (INH-SH) signal travels at the group velocity of the pump pulse. In a recent study phase and group velocity matching were demonstrated in lithium niobate in the range of transparency for all fields. The INH-SH was shown to refract at the same angle, and travel at the same velocity, as the pump.⁵ At the same time, the homogeneous SH component refracts and travels according to the values one expects from material dispersion at that frequency.

The inhomogeneous component is generally difficult to observe because it travels locked under the pump pulse, with relatively low conversion efficiencies. In a recent study the results were generalized to include third harmonic generation (THG) in both positive and negative index media.⁶ When a pump signal traverses an interface into a nonlinear medium it generates SH and/or TH fields. Each harmonic has two parts: (i) a homogeneous portion that walk-off from the pump field; (ii) an inhomogeneous component phase- and velocity-locked to the pump, with no energy transfer between the fields except at interface crossings. The key observation here is that the INH-SH has a k -vector always double that of the pump, even for large phase mismatches. Theoretical findings thus suggest that the INH-SH signal experiences an *effective complex index* of refraction given by $2k_{\omega}c/2\omega = k_{\omega}c/\omega = n_{\omega}$, i.e., the same index of refraction as the pump pulse.

In Ref. 7, a pump pulse tuned at 1300 nm was launched into a slab of GaAs 500 μm thick. Transmitted SH and TH signals were detected at 650 nm and 433 nm, respectively, far below the absorption band edge (~ 900 nm). Simulations showed that only the inhomogeneous components propagate. Further experimental evidence⁸ shows that the INH-SH is

enhanced by several orders of magnitude compared to bulk⁷ in an opaque GaAs cavity environment thanks to pump and INH-SH field localization and overlap.⁹ The results of more experiments carried out in a high-Q GaAs cavity¹⁰ hint that the INH-SH signal (612 nm) can achieve conversion efficiencies of order 10^{-3} with pumping intensities as low as 0.15 MW/cm² inside the cavity.

We now ask the following question: does this phenomenon hold for harmonic fields tuned at frequencies in the metallic range? In other words, will a harmonic field propagate if it happens to be tuned in a region where $\text{sign}(\epsilon) \neq \text{sign}(\mu)$, where one expects no propagating solutions? The short answer to this question is *yes*. In what follows we provide experimental and numerical evidence that show how an electromagnetic field is generated and propagates in otherwise forbidden wavelength ranges. In Fig. 1 we show the dispersion of GaP as given in Ref. 11. The pump pulse is tuned in the transparency region, at ~ 670 nm, where $\epsilon_{670 \text{ nm}} \approx 10.7$. SH and TH fields are tuned to 335 nm ($\epsilon_{335 \text{ nm}} = 19.1 + i24.1$) and 223 nm ($\epsilon_{223 \text{ nm}} = -9.6 + i10.4$, in the metallic range), respectively. With these dispersion values, two externally incident seed fields tuned at or below 335 nm would be completely reflected and/or absorbed within just a few nanometers from the surface. Below we show that the situation is dramatically different if nonlinear phenomena are considered.

The experimental setup used to measure transmitted harmonics in GaP is shown in Fig. 1. Incident 80 fs pulses centered at ~ 670 nm were generated by an optical parametric amplifier and amplified Ti:sapphire laser system operating at 1 kHz repetition rate. Prior to sending the pump beam into the experimental setup, an equilateral dispersing prism and spatial filtering were used to remove background harmonics present in the beam path. A color filter was placed directly before the sample to remove any residual harmonics. At the sample position, the collimated pump beam's pulse energy was 2.7 μJ , corresponding to a peak intensity of 480 MW/cm². After propagating through the sample, the residual pump was filtered and the harmonics were reflected by four long wave pass (LWP) dichroic beam splitters. The second (third) harmonic mirrors each transmitted $>90\%$ of the pump and reflected $>97\%$ ($>95\%$) of the harmonic. While propagating through the sequence of LWP mirrors, a

^{a)}Electronic mail: vito.roppo@upc.edu.

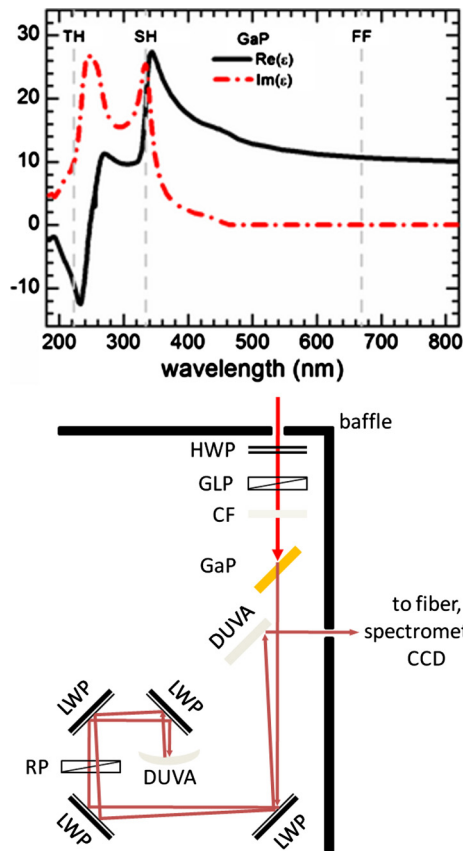


FIG. 1. (Color online) (Top) dispersion relation of GaP from Ref. 12. The dashed lines indicate tuning of the fields. There are two resonances, at ~ 330 and 240 nm. (Bottom) Experimental setup. The polarization of input pump pulses at 670 nm is set by a half-wave plate (HWP) and Glan-laser polarizer (GLP). A color filter (CF, Corning 3-73) removes the harmonics before the pumps strikes the GaP sample. The harmonics reflect off four LWP dichroic beam splitters. A Rochon polarizer (RP) transmits only one polarization of harmonic light. A concave aluminum mirror with deep-ultraviolet coating (DUVA) retroreflects the harmonic back through the RP/LWP system and focuses the harmonic into an all-silica fiber for detection.

single polarization of harmonic light was selected by a polarizer with single-pass extinction ratio of $\sim 10^{-3}$. Each harmonic was reflected back through the mirrors and polarizer by a concave aluminum mirror with deep-ultraviolet coating. Therefore, the residual pump light was suppressed by at least eight orders of magnitude and either the TM or TE component of the harmonic was selected with a contrast of at least 10^6 . After passing back through the mirrors and polarizer, the harmonic was focused into an all-silica fiber coupled to a UV-sensitive spectrometer and liquid nitrogen cooled charge-coupled device. In Fig. 2 we show the measured spectra (solid curves) for the case of a TM-polarized pump field. The $\langle 100 \rangle$ GaP $500 \mu\text{m}$ thick wafer was illuminated at 40° . The basic results may be summarized as follows: the harmonic conversion efficiencies for the transmitted fields are approximately 10^{-9} for the TE-polarized SH at 335 nm and $\sim 1.8 \times 10^{-12}$ for the TM-polarized TH at 223 nm. The detection limit of the system corresponds to a minimum detectable efficiency of $\sim 10^{-14}$. Any background harmonic present with the sample removed was below this detection limit.

We confirmed our experimental results by numerically solving Maxwell's equations in the time domain. The material was modeled as a collection of doubly resonant harmonic

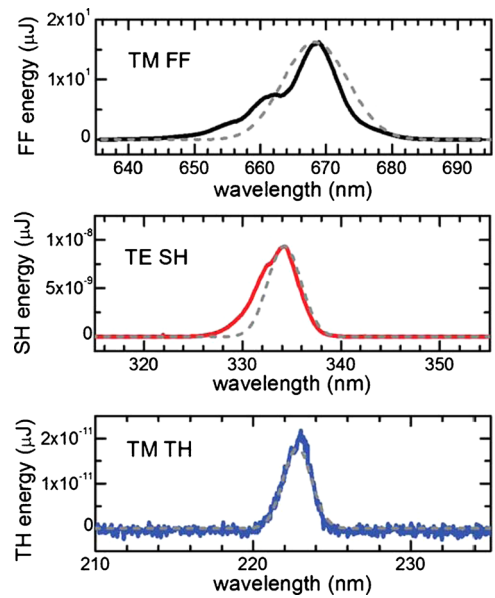


FIG. 2. (Color online) Measured spectra for the TM-polarized pump (continuous lines). Results of the numerical simulation (dashed lines).

oscillators (see Fig. 1) with a nonlinear polarization of the usual type: $\mathbf{P}_{NL} = \chi^{(2)}\mathbf{E}^2 + \chi^{(3)}\mathbf{E}^3$. The model is described in details in Refs. 12 and 13. As in Ref. 12 we also operate in a two-dimensional space, and allow the simultaneous presence of TE- and TM-polarized fields so that each has a two-dimensional spatial description. This wider theoretical description takes into account harmonic generation that arises from all interface crossings (spatial derivatives on the polarization vectors) and from the magnetic Lorentz force, which is usually neglected outside the context of metals. The total polarization that is fed back into Maxwell's equations is the vector sum of the polarization given by these nonlinear sources and the nonlinear polarization that arises from $\chi^{(2)}$ and $\chi^{(3)}$ phenomena.

When the pump is TM-polarized the $\chi^{(2)}$ tensor of GaP (the only nonzero components are $d_{14}=d_{25}=d_{36}$) selects the TE-polarized SH signal. Simulations show that only the INH-SH is left intact. Harmonic signals generated at the surface due to symmetry breaking have the same polarization as the incident pump pulse¹² but have much smaller conversion efficiencies compared to $\chi^{(2)}$ contributions. Thus, cross checking the polarization of the generated signal can be used to determine its origin, i.e., surface or bulk. Using the theoretical approach outlined in Ref. 12, we determined that the efficiency of the transmitted, surface-generated, TM-polarized SH field is of order 10^{-11} , or two orders of magnitude smaller than the TE-polarized component that arises from the $\chi^{(2)}$ tensor of the medium. The experiment confirms these findings. As a result, there is little doubt that most of the TE-polarized signal originates inside GaP.

For THG, nonlinear surface and volume sources that arise from Coulomb and magnetic Lorentz forces only¹² are inadequate to generate an observed transmitted, TM-polarized TH signal with an efficiency of 10^{-12} . Integrating Maxwell's equations *without* $\chi^{(2)}$ and $\chi^{(3)}$ contributions yields TH conversion efficiencies of order 10^{-20} . An adequate prediction of THG can be made by adopting a realistic third order $\chi^{(3)}$ tensor of cubic type, with $\bar{4}3m$ symmetry and four independent components, namely

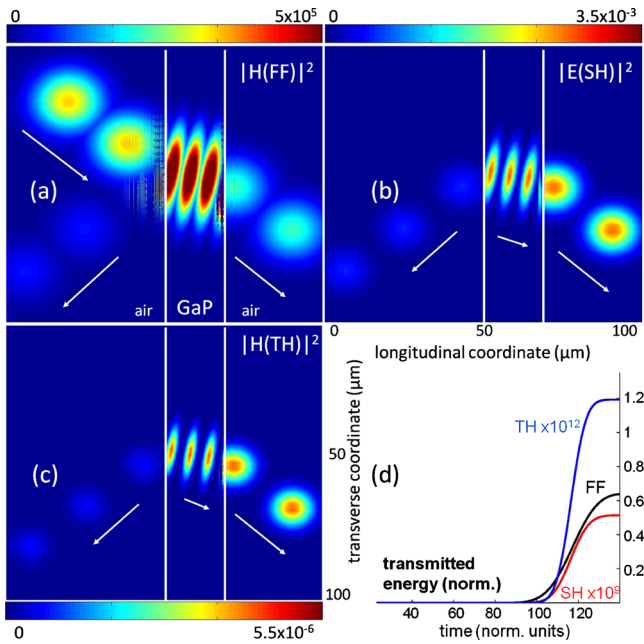


FIG. 3. (Color online) Time propagation that shows superposition of different temporal snapshots. An 80 fs pump pulse impinges at 40° on a GaP 20 μm thick slab (a) and SH (b) and TH (c) signals are generated. The harmonic signals keep propagating inside the bulk material perfectly overlapped to the pump pulse without being absorbed, quite insensitively to substrate thickness. (d) Field energies as a function of time at the right of the sample.

$\chi_{xxxx}^{(3)}, \chi_{yyyy}^{(3)}, \chi_{zzzz}^{(3)}, \chi_{yyyz}^{(3)}, \chi_{yzyz}^{(3)}$, with $\chi_{xxxx}^{(3)} = \chi_{yyyy}^{(3)} = \chi_{zzzz}^{(3)}$. The symmetry properties of the tensor for this class of materials may be consulted in Ref. 14. Our model thus includes surface and volume contributions from Coulomb and magnetic forces, and contributions from realistic nonlinear second and third order tensors that give rise to SHG and THG.

In Fig. 3, we show different temporal snapshots of incident and generated harmonic pulses. As the input pulse [Fig. 3(a)] enters the material SHG and THG occur. In the figure we report the most intense components, namely, TE-polarized SH [Fig. 3(b)] and TM-polarized TH [Fig. 3(c)] pulses. The homogeneous components quickly vanish due to either the high absorption (SH) or the metallic environment (TH). The inhomogeneous components are the only portions of the harmonics that survive, and they overlap the pump pulse at all times. The amount of energy transferred to each harmonic is dictated by the index mismatch at the interface, and does not vary during propagation.⁶ When the pump pulse reaches the exit surface the fields decouple and propagate freely. In Fig. 3(d), we show the transmitted field energies by monitoring them as a function of time (bottom right).

The calculated spectra are shown in Fig. 2 (dashed lines) and they overlap well the experimental data when we choose $\chi^{(2)} = 2d_{14} = 2d_{25} = 2d_{36} \approx 500$ pm/V, and $\chi_{xxxx}^{(3)} = \chi_{yyyy}^{(3)} = \chi_{zzzz}^{(3)} \approx 4 \times 10^{-19}$ m²/V². Although the remaining third order tensor components $\chi_{yyxx}^{(3)}, \chi_{yzyz}^{(3)}$ and $\chi_{yzyz}^{(3)}$ are also included in the calculation and are taken to be of the same order as the diagonal terms, in this single-interface environment they contribute little the overall TH conversion efficiency.

Beside some aspects that have fundamental relevance, the discovery that the phase locking phenomenon still applies in the UV regime for harmonics tuned in spectral

ranges where the medium displays metallic behavior may be of some technological importance in rethinking and redesigning semiconductor-based integrated devices at the nano-scale. Harmonic generation is only one aspect of the role that common semiconductors can play at UV wavelengths, i.e., ranges where typical semiconductors distinguish themselves only for their opacity. As another example, semiconductor-based superlenses¹⁵ and enhanced transmission gratings¹⁶ that operate in the UV range have already been proposed. Taken together, these results show that the functionality of semiconductors may be pushed down the wavelength scale, toward the soft x-ray region of the spectrum. The next step to take beyond this work is to study the dynamics in cavity environments, as was done previously,^{8,10} possibly in silicon or metal-semiconductor structures,¹² where the $\chi^{(3)}$ of metals can be fully exploited to achieve high conversion efficiencies in the deep UV range.

In summary, we have experimentally and theoretically demonstrated the propagation of light pulses in the ultraviolet metallic frequency range of GaP. The pulse was generated near the entry surface of the sample as a third harmonic signal using quadratic and cubic nonlinearities of the material. The propagation was made possible by a phase locking mechanism that binds inhomogeneous harmonic components to the fundamental field, an effect that persists regardless of the dispersive characteristics of the medium at the harmonic wavelengths.

V.R. acknowledges partial financial support from the Army Research Office (Grant No. W911NF-10-2-0105). N.A. acknowledges financial support provided by the National Research Council.

¹N. Bloembergen and P. S. Pershan, *Phys. Rev.* **128**, 606 (1962).

²W. Su, L. Qian, H. Luo, X. Fu, H. Zhu, T. Wang, K. Beckwitt, Y. Chen, and F. Wise, *J. Opt. Soc. Am. B* **23**, 51 (2006).

³L. D. Noordam, H. J. Bakker, M. P. de Boer, and H. B. van Linden van den Heuvel, *Opt. Lett.* **15**, 1464 (1990).

⁴M. Mlejnek, E. M. Wright, J. V. Moloney, and N. Bloembergen, *Phys. Rev. Lett.* **83**, 2934 (1999).

⁵E. Fazio, F. Pettazzi, M. Centini, M. Chauvet, A. Belardini, M. Alonzo, C. Sibilina, M. Bertolotti, and M. Scalora, *Opt. Express* **17**, 3141 (2009).

⁶V. Roppo, M. Centini, C. Sibilina, M. Bertolotti, D. de Ceglia, M. Scalora, N. Akozbek, M. J. Bloemer, J. W. Haus, O. G. Kosareva, and V. P. Kandidov, *Phys. Rev. A* **76**, 033829 (2007).

⁷M. Centini, V. Roppo, E. Fazio, F. Pettazzi, C. Sibilina, J. W. Haus, J. V. Foreman, N. Akozbek, M. J. Bloemer, and M. Scalora, *Phys. Rev. Lett.* **101**, 113905 (2008).

⁸V. Roppo, C. Cojocaru, F. Raineri, G. D'Aguzzo, J. Trull, Y. Halioua, R. Raj, I. Sagnes, R. Vilaseca, and M. Scalora, *Phys. Rev. A* **80**, 043834 (2009).

⁹V. Roppo, C. Cojocaru, J. Trull, R. Vilaseca, and M. Scalora, *Waves Random Complex Media* **20**, 319 (2010).

¹⁰V. Roppo, F. Raineri, R. Raj, I. Sagnes, J. Trull, R. Vilaseca, M. Scalora, and C. Cojocaru, "Enhanced efficiency of second harmonic inhomogeneous component in opaque cavity," *Opt. Lett.* (to be published).

¹¹E. D. Palik, *Handbook of Optical Constants of Solids* (Academic, New York, 1985), p. 350.

¹²M. Scalora, M. A. Vincenti, D. de Ceglia, V. Roppo, M. Centini, N. Akozbek, and M. J. Bloemer, *Phys. Rev. A* **82**, 043828 (2010).

¹³G. Burns, *Solid State Physics* (Academic, London, 1985), p. 511.

¹⁴R. W. Boyd, *Nonlinear Optics*, 2nd ed. (Academic, New York, 2003), p. 51.

¹⁵M. A. Vincenti, A. D'Orazio, M. G. Cappeddu, N. Akozbek, M. J. Bloemer, and M. Scalora, *J. Appl. Phys.* **105**, 103103 (2009).

¹⁶M. A. Vincenti, D. de Ceglia, M. Buncick, N. Akozbek, M. J. Bloemer, and M. Scalora, *J. Appl. Phys.* **107**, 053101 (2010).